Binuclear Platinum(II) Triazolopyrimidine Bridged Complexes. Preparation, Crystal Structure, NMR Spectroscopy, and ab Initio MO Investigation on the Bonding Nature of the Pt(II)···Pt(II) Interaction in the Model Compound $\{Pt_2[NHCHN(C(CH_2)(CH_3))]_4\}$

Jorge A. R. Navarro,[†] M. Angustias Romero,[†] Juan M. Salas,*[,†] Miguel Quirós,[†] Jaouad El Bahraoui,[‡] and José Molina[‡]

Departamento de Química Inorgánica and Laboratorio de Modelización y Diseño Molecular, Universidad de Granada, 18071 Granada, Spain

Received May 8, 1996[⊗]

A condensation reaction between two *cis*-$[PtCl_2(Hmtpo)_2]$ (where Hmtpo= 4,7-*H*-5-methyl-7-oxo[1,2,4]triazolo-[1,5a]pyrimidine) molecules takes place in neutral aqueous media, giving $[Pt_2(\mu\text{-mtpo})_4]\cdot 4H_2O$ (**1**). The X-ray structure of the recrystallization product of **1** in DMSO:EtOH (1:1) (DMSO = dimethyl sulfoxide), namely, $[Pt_2(\mu\text{-mtpo})_4]\cdot 2DMSO$ (**2**) has been determined. Compound **2** crystallizes in the orthorhombic space group *Pbcn* with unit cell dimensions $a = 14.207(3)$ Å, $b = 15.187(3)$ Å, $c = 17.165(3)$ Å, and $Z = 4$. The molecular structure shows that the two Pt atoms are bridged by four mtpo ligands. Thus, it presents two face to face PtN_4 units with a Pt···Pt 2.744(2) Å separation. Compound **1** has also been characterized by ^1H and ^{195}Pt NMR. The very short Pt(II)···Pt(II) contact suggests an interaction between the two metal centers, supported by the great deshielding observed for the platinum nuclei in the ^{195}Pt NMR spectrum ($\delta = -2005$ ppm) compared to a Pt(II) in a typical N_4 environment. In order to make an approach to the possible bonding nature of the Pt(II)···Pt(II) interaction, a theoretical analysis has been performed on the basis of the properties of the electronic charge density distribution, derived from ab initio MO calculations for the model compound $\{Pt_2[NHCHN(C(CH_2)(CH_3))]_4\}$ using RHF/LANL2DZ and B3LYP/LANL2DZ wave functions; both take into account relativistic effects and the second electronic correlation also. A significant directional interaction between the two metal centers has been found. Thus, a bond critical point appears between the two platinum nuclei, with a density of charge $\rho_b = 0.056$ e·bohr^{-3}, which is half of that found for the platinum nitrogen bond. Moreover, a value of the energy density, $E_d(r_b) < 0$ ($E_d(r) = -0.0175$ hartree·bohr^{-3}), at this point, shows the bonding nature of the interaction.

Introduction

Association of square-planar complexes of Pt(II) and other d^8 metal ions in pairs or stacks is a well-known phenomenon, both in the solid state[1,2] and in solution.[3,4] These compounds present M···M contacts in the range 2.6−3.5 Å, which is shorter than the sum of van der Waals radii. This association appears to be a key step in the formation of one-dimensional materials such as Pt mixed valence complexes.[1,2] One of the most interesting subjects of research in this field has been the chemistry of *cisplatin* and related compounds. Apart from the anticarcinogenic properties of these compounds,[5] they have been used with the help of secondary bridging ligands such as α-pyridone, α-pyrrolidone, 1-methyluracil, 1-methylcitosine, and analogous compounds, to prepare homo-[1,6] and heteronuclear[7] complexes. The resulting polynuclear compounds display interesting properties due to the short M−M contacts, such as photochemical properties,[8] stabilization of rare states of oxidation for platinum[9] and palladium,[10] or the utilization of the platinum nucleus as a weak σ-donor ligand in the coordination chemistry of metal ions.[11]

The present paper reports the ability of a *cisplatin* analogue, namely, *cis*-$[PtCl_2(Hmtpo\text{-}N(3))_2]$[12] (where Hmtpo = 4,7-*H*-5-methyl-7-oxo[1,2,4]triazolo[1,5a]pyrimidine) for generating platinum binuclear complexes. This compound presents the interesting feature that the nitrogen donor ligand is able to participate as a bridging ligand. Thus, it is possible to get a tetrabridged platinum binuclear complex $[Pt_2(\mu\text{-mtpo-}N(3),N(4))_4]$ (Figure 1a), with an intermetallic distance ($d_{Pt-Pt} = 2.744(2)$ Å) much shorter than the doubly bridged compounds achieved from *cisplatin*.[1]

[†] Departamento de Química Inorgánica.
[‡] Laboratorio de Modelización y Diseño Molecular.
[⊗] Abstract published in *Advance ACS Abstracts,* November 15, 1996.

(1) (a) Hollis, L. S.; Lippard, S. J. *J. Am. Chem. Soc.* **1981,** *103,* 1230. (b) Trötscher, G.; Micklitz, W.; Schöllhorn, H.; Thewalt, U.; Lippert, B. *Inorg. Chem.* **1990,** *29,* 2541.
(2) Miller, J. S.; Epstein, A. J. *Prog. Inorg. Chem.* **1976,** *20,* 1.
(3) Bailey, J. A.; Hill, M. G.; Marsh, R. E.; Miskowski, V. M.; Schaefer, W. P.; Gray, H. B. *Inorg. Chem.* **1995,** *34,* 4591.
(4) Jennette, K. W.; Gill, J. T.; Sadownick, J. A.; Lippard, S. J. *J. Am. Chem. Soc.* **1976,** *98,* 6159.
(5) Rosenberg, B.; vanCamp, L.; Trosko, J. F.; Mansour, V. H. *Nature* **1969,** *222,* 385.
(6) (a) Schöllhorn, H.; Thewalt, U.; Lippert, B. *Inorg. Chim. Acta* **1984,** *93,* 19. (b) Faggiani, R.; Lippert, B.; Lock, C. J. L.; Speranzini, R. A. *J. Am. Chem. Soc.* **1981,** *103,* 1111. (c) Matsumoto, K.; Harashima, K.; Moriyama, H.; Sato, T. *Inorg. Chim. Acta* **1992,** *197,* 217.
(7) (a) Micklitz, W.; Riede, J.; Huber, B.; Müller, G.; Lippert, B. *Inorg. Chem.* **1988,** *27,* 1979. (b) Lippert, B.; Schöllhorn, H.; Thewalt, U. *Inorg. Chem.* **1987,** *26,* 1736.
(8) Yip, H.-K.; Che, C. M.; Zhou, Z.-Y.; Mak, T. C. W. *J. Chem. Soc., Chem. Commun.* **1992,** 1369.
(9) (a) Barton, J. K.; Rabinowitz, H. N.; Szalda, D. J.; Lippard, S. J. *J. Am. Chem. Soc.* **1977,** *99,* 2827. (b) Sakai, K.; Matsumoto, K. *J. Am. Chem. Soc.* **1989,** *111,* 3074. (c) Matsumoto, K.; Takabashi, H.; Fuwa, K. *J. Am. Chem. Soc.* **1984,** *106,* 2049. (d) Renn, O.; Albinati, A.; Lippert, B. *Angew. Chem., Int. Ed. Engl.* **1990,** *29,* 84. (e) Lippert, B.; Schöllhorn, H.; Thewalt, U. *J. Am. Chem. Soc.* **1986,** *108,* 525.
(10) Micklitz, W.; Müller, G.; Huber, B.; Riede, J.; Rashwan, F.; Heinze, J.; Lippert, B. *J. Am. Chem. Soc.* **1988,** *110,* 7084.
(11) (a) Goodgame, D. M. L.; Hitchman, M. A.; Lippert, B. *Inorg. Chem.* **1986,** *25,* 2191. (b) Duckworth, D. M.; Goodgame, D. M. L.; Hitchman, M. A.; Lippert, B.; Murray, K. S. *Inorg. Chem.* **1987,** *26,* 1823.
(12) Rodríguez, J.; Salas, J. M.; Romero, M. A.; Quirós, M.; Faure, R. *J. Inorg. Biochem.* **1995,** *59,* 223.

S0020-1669(96)00496-X CCC: $12.00

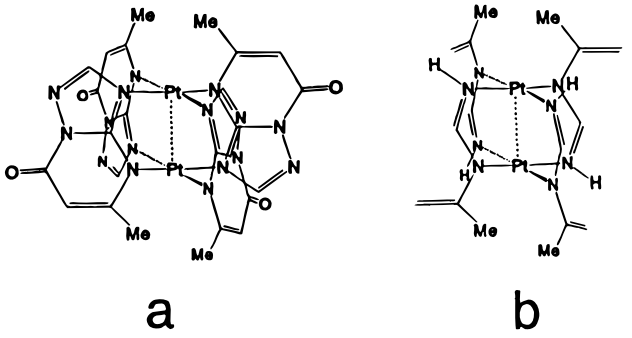

Figure 1. $[Pt_2(\mu\text{-mtpo})_4]$ (a) and model system $\{Pt_2[NHCHN(C(CH_2)(CH_3))]_4\}$ (b).

Chart 1

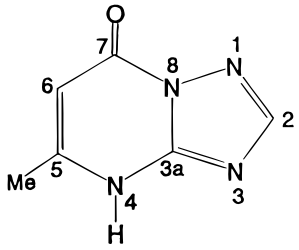

The heterocyclic Hmtpo ligand (Chart 1) is ideally suited for the preparation of multinuclear metal complexes and study of M−M interactions, providing at least four potential binding sites, one of which (N4) requires deprotonation prior to metal ion coordination. In previous studies, this ligand has exhibited a monodentate (via N3) coordination mode in two monomeric Cu(II) complexes[13] and multidentate behavior with participation of N(1), N(3), N(4), and O(7) as donor sites in a polymeric Ag(I) complex.[14]

The dynamic electronic correlation effects, which make accurate calculations based on Hartree−Fock approximation so difficult for transition metal complexes, appear to be treated reasonably accurately with the new generation of "gradient corrected" density functional theories (DFT).[15] Thus, some authors have obtained accurate results with this approach in the study of the binding energies of some metal complexes and inorganic compounds.[16] Moreover, for heavy metal ions the effect of relativity plays an important role. Thus, the use of effective core potentials (ECPs), which replace the core electrons, incorporate the effects of relativity, reducing the size of the basis set to treat the molecule.

Furthermore, Bader has introduced a theoretical approach based on his theory of atoms in molecules[17] in which all information of the system is deduced from the properties of the molecular electronic charge density. Thus, in order to discern the nature of the M−M interaction in $[Pt_2(\mu\text{-mtpo})_4]$ a topological study of the electronic charge distribution for the model compound $\{Pt_2[NHCHN(C(CH_2)(CH_3))]_4\}$ (Figure 1b) has been carried out.

(13) Dirks, E. J.; Haasnoot, J. G.; Kinneging, A. J.; Reedijk, J. *Inorg. Chem.* **1987,** *26*, 1902.
(14) Smith, D. L. and Luss, H. R. *Photogr. Sci. Eng.* **1976,** *20*, 184.
(15) (a) Parr, R. G.; Yang, W. *Density Functional Theory of Atoms and Molecules*; Oxford University Press: Oxford, U.K., 1989. (b) Ziegler, T. *Chem. Rev.* **1991,** *91*, 651. (c) Johnson, B. G.; Gill, P. M. W.; Pople, J. A. *J. Chem. Phys.* **1993,** *98*, 5612.
(16) (a) Ricca, A.; Bauslicher, C. W. *J. Phys. Chem.* **1994,** *98*, 12899. (b) Russo, T. V.; Martin, R. L.; Hay, P. J. *J. Phys. Chem.* **1995,** *99*, 17085.
(17) Bader, R. F. W. *Atoms in Molecules: A Quantum Theory*; Clarendon Press: Oxford, U.K., 1990.

Table 1. Crystallographic Data for $[Pt_2(\mu\text{-mtpo})_4]\cdot 2DMSO$ (**2**)

formula	$C_{28}H_{32}N_{16}O_6Pt_2S_2$	Z	4
fw, g/mol	1142.4	μ, cm^{-1}	77
space group	*Pbcn* (No. 60)	T, °C	20
a, Å	14.207(3)	λ, Å	0.710 73
b, Å	15.187(3)	ρ_{obs}, g cm^{-3}	$2.06\cdot\rho_{calc} = 2.050$
c, Å	17.165(3)	$R(F_o)^a$	0.093 ($I > 2\sigma(I)$)
V, Å^3	3704(1)	$R_w(F_o^2)^b$	0.154 (all data)

^{a} $R = \sum||F_o| - |F_c||/\sum|F_o|$. ^{b} $R_w = [\sum w[(F_o^2 - F_c^2)^2]/\sum(wF_o^4)]^{1/2}$; $w = 1/[s^2(F_o)^2 + (0.0488P)^2]$, where $P = (F_o^2 + 2F_c^2)/3$.

Experimental Section

Reactants and Methods. *cis*-$[PtCl_2(Hmtpo\text{-}N(3))_2]\cdot 3H_2O$ was prepared as previously reported.[12] 4,7-H-5-Methyl-7-oxo[1,2,4]triazolo-[1,5a]pyrimidine was purchased from Aldrich Chemical Co. and used as received. The other chemical reagents and solvents were supplied from commercial sources. All experiments were performed in air.

Preparation of $[Pt_2(\mu\text{-mtpo-}N(3),N(4))_4]\cdot 4H_2O$, 1. A suspension of *cis*-$[PtCl_2(Hmtpo\text{-}N(3))_2]\cdot 3H_2O$ (1.200 g, 1.93 mmol) in water (20 mL) was solubilized by adjusting the pH to 7 with NaOH (1 N). The resulting clear yellow solution was refluxed and stirred for 63 h, giving a pale yellow precipitate and a mother liquor with a lower pH (pH = 4.4). The precipitate was washed with water, with ethanol, and finally with ether and dried overnight at 45 °C. Adjusting the mother liquor to pH 7 and refluxing for 24 h gives a smaller second fraction of the precipitate; yield, 49%. Anal. Calcd (found) for $C_{24}H_{28}N_{16}O_8Pt_2$: C, 27.2 (27.1); H, 2.6 (2.5); N, 21.2 (21.2); Pt, 36.5 (35.5). IR (cm^{-1}): 572 m, 1026 m, 1148 m, 1207 m, 1387 m, 1422 s, 1534 vs, 1591 m, 1682 vs, 3430 s. ^{1}H NMR (DMSO-d_6; ppm): δ 8.55 (s, 1H, H(2)), 5.84 (s, 1H, H(6)), 3.05 (s, 3H, Me). ^{195}Pt NMR (DMSO-d_6; ppm): δ −2005 (s).

Preparation of $[Pt_2(\mu\text{-mtpo-}N(3),N(4))_4]\cdot 2DMSO$, 2. $[Pt_2(\mu\text{-mtpo-}N(3),N(4))_4]\cdot 4H_2O$ (0.160 g, 0.150 mmol) was suspended in DMSO:EtOH (1:1, 20 mL) and was heated until all of the material was dissolved. The resulting yellow solution gave after 3 weeks a small amount of prismatic yellow crystals. Elemental analysis data of single crystals of **2** (found: C, 28.4; H, 2.9; N, 18.4; S, 6.0) fit the description as dihydrate better than as anhydrate in accord with the X-ray results. Calcd for $C_{28}H_{36}N_{16}O_8S_2Pt_2$: C, 28.3; H, 3.1; N, 18.9; S, 5.4. ^{1}H NMR (DMSO-d_6; ppm): δ 8.55 (s, 1H, H(2)), 5.84 (s, 1H, H(6)), 3.05 (s, 3H, Me).

Instrumentation. Microanalysis of C, H, N, and S were performed with a Fisons-Instruments EA-1008 by the Instrumentation Center of the University of Granada. Infrared spectra were recorded in the 180−4000 cm^{-1} range on a Perkin-Elmer 983G spectrophotometer, using KBr and polyethylene pellets. Thermogravimetric (TG) diagrams were obtained on Mettler TA-3000 equipment provided with a Mettler TG-50 thermobalance at a heating rate of 20 K min^{-1}, using an atmosphere of pure air (100 mL min^{-1}). NMR studies were carried out in the Department of Chemistry of the University of Dortmund, recorded on a Bruker AC-200 FT NMR spectrometer. ^{1}H NMR spectra were recorded in DMSO-d_6 with TMS as internal standard. ^{195}Pt NMR spectra were recorded in DMSO-d_6 (D_2O, external K_2PtCl_4 reference). Reported shifts are relative to $[PtCl_6]^{2-}$.

Oxidation Studies. Ce(IV) tritations of **1** were carried out in 0.7 M H_2SO_4 with $Ce(SO_4)_2$ (dissolved in 0.7 M H_2SO_4). The concentration of the complex was 2×10^{-3} M and that of Ce(IV) was 5×10^{-2}. The Pt combination electrode (Metrohm, Ag/AgCl reference) used to monitor the redox reactions was standardized in a solution of chinhydrone in a pH 4 buffer ($E = 259 \pm 5$ mV).

X-ray Crystallography. Relevant crystallographic data and details of refinement for **2** are presented in Table 1. A crystal, of dimensions $0.08 \times 0.1 \times 0.5$ mm, was mounted on a Stoe-Siemens AED-2 diffractometer. A total of 3660 unique reflection intensities were measured in the range $3 < 2\theta < 60°$. The intensity data were corrected for Lorentz and polarization effects and empirically (ψ scans) for absorption (transmission range is 0.17−0.13). The structure was solved by the heavy atom and Fourier methods applying the SHELXTL PLUS

program package.[18] Full matrix least-squares refinement (on F^2) was performed with anisotropic thermal parameters for non-hydrogen atoms with the exception of the DMSO molecules (the two DMSO molecules were found to be disordered in two positions with occupancies of $^1/_2$ each) using the SHELX-93 program package.[19]

Computational (MO Calculation) Work. Ab initio MO calculations for the model compound $\{Pt_2[NHCHN(C(CH_2)(CH_3))]_4\}$ (Figure 1b) have been performed through the GAUSSIAN-94 Revision C.2 series program[20] using restricted Hartree−Fock (RHF) and density functional theory[15] (DFT) on a SGI Power Challenger machine. Among the characteristics of this code are the use of Gaussian basis functions, the avoidance of auxiliary functions, the implementation of large grids, and the availability of analytical first and second derivatives.[21]

In hybrid methods the exchange-correlation energy (E_{xc}) is represented by the following general equation:

$$E_{xc} = a_0 E_x^{UEG} + (1 - a_0)E_x^{HF} + a_x \Delta E_x + E_c^{UEG} + a_c \Delta E_c \quad (1)$$

where E_x^{UEG} is the density functional for the exchange energy of the uniform electron gas,[22] E_c^{UEG} the corresponding correlation contribution,[23] E_x^{HF} is the Hartree−Fock exchange, and the ΔE terms are the gradient correction contributions to exchange and correlation. A hybrid method is further qualified as self-consistent when gradient correction and HF exchange are not simply computed using a converged LSD wave function (or, more traditionally, LSD and gradient correct contributions added to a converged HF wave function), but the SCF process is performed with the complete density functional. The B3LYP variant is obtained using the Becke gradient correction to exchange,[24] and the Lee−Yang−Parr (LYP) correlation functional.[25] Since the LYP functional contains both a local part and a gradient correction, only the latter contribution should be used to obtain a coherent implementation. It is, however, expedient to use the approximation

$$\Delta E_c \approx E_c^{LYP} - E_c^{VWN}$$

A number of tests showed that values of the three semiempirical coefficients appearing in eq 1 near 0.80 provide the best results, irrespective of the particular form of the different functionals. The values ($a_0 = 0.80$, $a_x = 0.72$, $a_c = 0.81$) determined by Becke from a best fitting of the heats of formation of a standard set of molecules[26] have been used.

Full geometry optimization for $\{Pt_2[NHCHN(C(CH_2)(CH_3))]_4\}$ was carried out by taking the experimental geometry of $[Pt_2(\mu\text{-mtpo})_4]$, keeping the original C_i symmetry. The LANL2DZ basis set has been used throughout the calculation which uses D95[27] at first and Hay and Wadt's large-core quasirelativistic effective core potential (LANL2)[28] on the Pt atom.

(18) Sheldrick, G. M. *SHELXTL PLUS*, Program Package for the Solution of Crystal Structures, Release 34; Siemens Analytical X-Ray Instruments Inc.: Madison, WI, 1989.
(19) Sheldrick, G. M. *SHELX-93*; University of Göttingen: Göttingen, Germany, 1993.
(20) Frisch, M. J.; Trucks, G. W.; Schlegel, H. B.; Gill, P. M. W.; Johnson, B. G.; Robb, M. A.; Cheeseman, J. R.; Keith, T. A.; Petterson, G. A.; Montgomery, J. A.; Raghavachari, K.; Al-Laham, M. A.; Zakrzewski, V. G.; Ortiz, J. V.; Foresman, J. B.; Cioslowski, J.; Stefanov, B. B.; Nanayakkara, A.; Challacombe, M.; Peng, C. Y.; Ayala, P. Y.; Chen, W.; Wong, M. W.; Andres, J. L.; Replogle, E. S.; Gomperts, R.; Martin, R. L.; Fox, D. J.; Binkley, J. S.; Defrees, D. J.; Baker, J.; Stewart, J. P.; Head-Gordon, M.; Gonzalez, C.; Pople, J. A. *Gausian 94*, Revision A.1; Gaussian Inc.: Pittsburgh, PA, 1992.
(21) (a) Gill, P. M. W.; Johnson, B. G.; Pople, J. A. *Chem. Phys. Lett.* **1993,** *209*, 506. (b) Johnson, B. G.; Frish, M. J. *J. Chem. Phys.* **1994,** *100*, 7429.
(22) Dirac, P. M. A. *Proc. Cambridge Philos. Soc.* **1930,** *26*, 376.
(23) Vosko, S. H.; Wilk, L.; Nsair, M. *Can. J. Phys.* **1980,** *58*, 1200.
(24) Becke, A. D. *Phys. Rev. B* **1988,** *38*, 3098.
(25) Lee, C.; Yang, W.; Parr, R. G. *Phys. Rev. B* **1988,** *37*, 785.
(26) Becke, A. D. *J. Chem. Phys.* **1993,** *98*, 5648.
(27) Dunning, T. H., Jr.; Hay, P. J. In *Modern Theoretical Chemistry*; Schaefer, H. F., III, Ed.; Plenum: New York, 1976; p 1−28.
(28) Schwerdtfeger, P.; McFeaters, J. S.; Moore, J. J.; McPherson, D. M.; Cooney, R. P.; Bowmaker, G. A.; Dolg, M.; Andrae, D. *Langmuir* **1991,** *7*, 116.

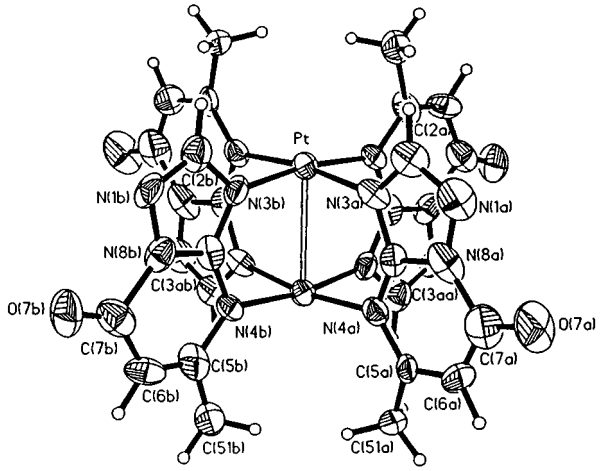

Figure 2. Molecular structure of $[Pt_2(\mu\text{-mtpo})_4]\cdot 2DMSO$. Thermal ellipsoids are drawn at the 30% probability level. The two disordered DMSO solvation molecules are not drawn.

Topological analysis of the charge density was performed by means of the AIMPAC series of programs[29] with the GAUSSIAN-94 results as input. Representation has been realized in the plane defined by C(3aA), C(3aB), C(3aA)′, C(3aB)′, and the plane defined by one of the two $Pt_2N_4C_2$ rings.

Results and Discussion

Solubilization of *cis*-$[PtCl_2(Hmtpo\text{-}N(3))_2]$ was accomplished after deprotonation of Hmtpo ligands by treatment with NaOH (1 N) until pH = 7. The deprotonation of the ligand activates the N(4) position, facilitating its possible involvement in a nucleophilic attack. Thus, when the solution is refluxed for a long time, a condensation reaction takes place between two *cis*-$[PtCl_2(mtpo\text{-}N(3))_2]^{2-}$ species (or any of its hydrolysis products) giving the dimeric compound $[Pt_2(\mu\text{-mtpo-}N(3),N(4))_4]\cdot 4H_2O$ (**1**) (Figure 1a). Compound **1** remains unaltered in air for several months. Thermogravimetric analysis of **1** shows that after the dehydration process (60−110 °C) it is thermally stable up to 400 °C.

Recrystallization of **1** from EtOH/DMSO (1:1) gave $[Pt_2(\mu\text{-mtpo-}N(3),N(4))_4]\cdot 2DMSO$ (**2**), the structure of which was studied by X-ray crystallography.

X-ray Structure of $[Pt_2(\mu\text{-mtpo})_4]\cdot 2DMSO$ (2). The molecular structure of **2** is shown in Figure 2. Crystal data are collected in Table 1, and selected interatomic distances and angles are listed in Table 2.

The structure consists of centrosymmetric dimeric $[Pt_2(\mu\text{-mtpo-}N(3),N(4))_4]$ units, in which the four mtpo ligands bridge the two platinum atoms, and disordered DMSO solvation molecules.

The coordination geometry of the metal atoms is square-pyramidal. The basal positions are occupied by four N-mtpo donor groups and the apical site by the other metal center of the dimer. The equatorial PtN_4 square has the *cis* configuration, which is consistent with the preparation method. Both platinum atoms are directed away from each other; deviations from the respective equatorial positions are 0.14 Å. The Pt−N distances are in good agreement with the values found for other platinum complexes with similar ligands.[30]

(29) Biegler-König, F. W.; Bader, R. F. W.; Tang, T. H. *J. Comput. Chem.* **1982**, *3*, 317.

Table 2. Comparison of Geometries for X-ray $[Pt_2(\mu\text{-mtpo})_4]\cdot 2DMSO$ (**2**) and Geometrical Optimization for Model Compound $[Pt_2\{NHCHN[C((CH_2)(CH_3))]\}_4]$ by RHF/LANL2DZ and B3lyp/LANL2DZ Methods[a]

	X-ray	RHF/LANL2DZ	B3lyp/LANL2DZ
	Bond Distances (Å)		
Pt−Pt′	2.743(2)	2.754	2.751
Pt−N(3A)	2.00(2)	2.069	2.049
Pt−N(3B)	1.95(2)	2.069	2.049
Pt−N(4A)′	2.05(2)	2.095	2.086
Pt−N(4B)′	2.06(2)	2.094	2.086
N(3A)−C(3aA)	1.38(3)	1.317	1.336
C(3aA)−N(4A)	1.31(3)	1.327	1.346
N(3B)−C(3aB)	1.35(3)	1.317	1.336
C(3aB)−N(4B)	1.36(3)	1.327	1.346
	Bond Angles (deg)		
N(3A)−Pt−N(3B)	87.9(7)	89.82	90.33
N(3A)−Pt−N(4B)′	89.9(7)	89.59	89.57
N(3A)−Pt−N(4A)′	171.6(8)	169.20	169.99
N(3B)−Pt−N(4A)′	89.5(7)	89.55	89.56
N(3B)−Pt−N(4B)′	171.0(7)	169.20	170.00
N(4A)′−Pt−N(4B)′	91.8(6)	89.01	88.81
N(4A)−C(3aA)−N(3A)	132(2)	126.91	126.56
C(3aA)−N(3A)−Pt	122(2)	125.47	125.15
C(3aA)−N(4A)−Pt′	114(2)	118.36	118.19
N(3A)−Pt−Pt′	83.1(6)	82.20	82.86
N(4A)−Pt′−Pt	88.5(7)	87.15	87.12
N(3B)−C(3aB)−N(4B)	128(2)	126.92	126.56
C(3aB)−N(3B)−Pt	125(2)	125.50	125.15
C(3aB)−N(4B)−Pt′	117(1)	118.32	118.19
N(3B)−Pt−Pt′	84.1(6)	82.17	82.87
N(4B)−Pt′−Pt	86.9(5)	87.07	87.19

[a] Prime indicates $-x, -y, -z$.

The most interesting feature in this complex is the short Pt(II)···Pt(II) contact ($d_{Pt-Pt} = 2.744(2)$ Å), being 0.7−0.9 Å shorter than the van der Waals radii sum[31] and close to the Bragg−Slater radii sum.[32]

The mtpo ligands are almost planar, with the methyl group 0.14 Å away from the least-squares plane, this fact being a consequence of the steric interaction with the methyl group of the other mtpo moiety (distance C(51A)−C(51B), 3.78 Å).

The two disordered DMSO molecules show only van der Waals interactions with the complex while $[Pt_2(\mu\text{-mtpo})_4]$ molecules in the crystal stack by interaction of the mtpo ligands labeled "B" (separation, 3.37 Å).

The Pt(II)···Pt(II) separation found in other platinum (II) tetrakis-bridged dimeric compounds are as follows: 2.649(1) Å for $[Pt_2(N,N'\text{-diphenylformamidinato})_4]$,[33] 2.680(2) Å for $[Pt_2(4\text{-methylpyridine-2-thiolato})_4]$,[34] 2.767(1) Å for $[Pt_2(CH_3CSS)_4]$,[35] 2.795(2) Å for $[Pt_2((CH_3)_2CHCSS)_4]$,[36] and 2.925(1) Å for $K_4[Pt_2(diphosphite)_4]\cdot 2H_2O$.[37] The Pt···Pt distance in our compound is within this range. The close approach of metal atoms in all of these complexes is supported by the presence of four bridging ligands. However, the intermetallic separation for **2** is considerably longer than the N−C−N bite of mtpo ligands, which is 2.45 Å. This increase may not be attributed to steric interactions between both metal centers, but to the steric demand of the triazolo ring annelated to the pyrimidine, since the donor orbitals of N(3) and N(4) are not parallel. This behavior is also observed in Ag(I)[38] and Cu(I)[39] dimers with analogous ligands, which display longer metal−metal distances than those found in compounds with ligands built by two annelated six-membered rings.[40] Thus, Pt···Pt separation for $[Pt_2(CH_3CSS)_4]$ is 0.17 Å shorter than the distance between the centers of the S_4 coordination planes,[35] while for $[Pt_2(N,N'\text{-diphenylformamidinato})_4]$ and $[Pt_2(4\text{-methylpyridine-2-thiolato})_4]$, in spite of the short intermetallic distance, there is no appreciable distortion from the square-planar geometry around the metal centers. Both facts suggest that a significant M−M interaction takes place, which allows the two metal centers to optimize their interatomic distances.

However, a diminution in the number of bridging ligands or their absence in Pt(II) dimers makes the intermetallic distance longer, in the range 2.9−3.1 Å [6,41] for covalently bridged dimers and 3.2−3.3 Å for the unbridged ones.[3,42] It should be noted that in the two latter sets of compounds, extra torsional strains are introduced by the nonbridging interligand interactions, which have an important role modulating the intermetallic separation.

In order to discern the nature of the Pt···Pt interaction in this compound, ^{195}Pt NMR studies have been carried out for **1** as well as molecular orbital calculations for the model compound $\{Pt_2[NHCHN(C(CH_2)(CH_3))]_4\}$.

NMR Studies. (i) ^{1}H NMR Spectroscopy. The ^{1}H NMR spectrum of **1** in DMSO-d_6 is indicative of complex formation. It consists of three peaks only, suggesting the equivalence of the four mtpo ligands in solution. ^{1}H NMR resonances of H(2) and CH_3 appear, respectively, 0.35 and 0.72 ppm deshielded with respect to free Hmtpo, while H(6) appears unaltered. Platinum binding to the N(3) position results in a downfield shift of H(2), in a way similar to that of purine bases H(8) after metal binding to N(7).[43] The large downfield shift of CH_3 is a consequence of the methyl disposition over the platinum coordination plane after binding to N(4). This fact may be diagnostic of the involvement of N(4) in the coordination of a d^8 metal ion,[44] and it may also be indicative of a weak Pt−H interaction (Pt···H separation, about 2.7 Å).[45,46]

(ii) ^{195}Pt NMR Spectra. The ^{195}Pt NMR spectrum of **1**

(30) (a) Sherman, S. E.; Gibson, D.; Wang, H. J.; Lippard, S. J. *J. Am. Chem. Soc.* **1988,** *110,* 7368. (b) Barnham, K. J.; Bauer, C. J.; Djuran, M. I.; Mazid, M. A.; Rau, T.; Sadler, P. J. *Inorg. Chem.* **1995,** *34,* 2826. (c) Frommer, G.; Mutikainen, I.; Pesch, F. J.; Hillgeris, E. C.; Preut, H.; Lippert B. *Inorg. Chem.* **1992,** *31,* 2429. (d) Schröder, G.; Lippert, B.; Sabat, M.; Lock, C. J. L.; Faggiani, R.; Song, B.; Sigel, H. *J. Chem. Soc., Dalton Trans.* **1995,** 3767.

(31) Bondi, A. *J. Phys. Chem.* **1964,** *68,* 441.

(32) Slater, J. C. *J. Chem. Phys.* **1964,** *41,* 3199.

(33) Cotton, F. A.; Matonic, J. H.; Murillo, C. A. *Inorg. Chem.* **1996,** *35,* 498.

(34) Umakoshi, K.; Kinoshita, I.; Ichimura, A.; Ooi, S. *Inorg. Chem.* **1987,** *26,* 3551.

(35) Bellitto, C.; Flamini, A.; Piovesana, O.; Zanazzi, P. F. *Inorg. Chem.* **1980**, *19,* 3632.

(36) Bellitto, C.; Dessy, G.; Fares, V.; Flamini, A. *J. Chem. Soc., Chem. Commun.* **1981,** 409.

(37) Filomena Dos Remedios Pinto, M. A.; Sadler, P. J.; Neidle, S.; Sanderson, M. R.; Subbiah, A.; Kuroda, R. *J. Chem. Soc., Chem. Commun.* **1980,** 13.

(38) (a) Gagnon, C.; Hubert, J.; Rivest, R.; Beauchamp, A. L. *Inorg. Chem.* **1977,** *16,* 2469. (b) Romero, M. A.; Salas, J. M.; Quirós, M.; Sánchez, M. P.; Molina, J.; El Bahraoui, J.; Faure, R. *J. Mol. Struct.* **1995,** *354,* 189.

(39) Haasnoot, J. G.; Favre, T. L. F.; Hinrichs, W.; Reedijk, J. *Angew. Chem., Int. Ed. Engl.* **1988,** *27,* 856.

(40) Munakata, M.; Maekawa, M.; Kitakawa, S.; Adachi, M.; Masuda, H. *Inorg. Chim. Acta* **1990,** *167,* 181.

(41) (a) Hollis, L. S.; Lippard, S. J. *J. Am. Chem. Soc.* **1983,** *105,* 3494. (b) Trovo, G.; Bandoli, G.; Casellato, U.; Corain, B.; Nicolini, M.; Longato, B. *Inorg. Chem.* **1990,** *29,* 4616. (c) Ratilla, E. M. A; Scott, B. K.; Moxness, M. S.; Kostic, N. M. *Inorg. Chem.* **1990,** *29,* 918. (d) Appleton, T. G.; Barnham, K. J.; Byriel, K. A.; Hall, J. R.; Kennard, C. H. L.; Mathieson, M. T.; Penman, K. G. *Inorg. Chem.* **1995,** *34,* 6040.

(42) (a) Cini, R.; Fanizzi, F. P.; Intini, F. P.; Maresca, L.; Natile, G. *J. Am. Chem. Soc.* **1993,** *115,* 5123. (b) Bardwell, D. A.; Crossley, J. G.; Jeffery, J. C.; Orpen, G.; Psillakis, E.; Tilley, E. E. M.; Ward, M. D. *Polyhedron* **1994,** *13,* 2291. (c) Kato, M.; Sasano, K.; Kosuge, C.; Yamazaki, M.; Yano, S.; Kimura, M. *Inorg. Chem.* **1996,** *35,* 116.

(43) Lippert, B. *Prog. Inorg. Chem.* **1989,** *37,* 1.

(44) Rodríguez, J. A.; Romero, M. A.; Salas, J. M.; Quirós, M. Submitted for publication.

(45) Miller, R. G.; Stauffer, R. D.; Fahey, D. R.; Parnell, D. R. *J. Am. Chem. Soc.* **1970,** *92,* 1511.

shows only one resonance peak, indicating the equivalence of both metal centers. ^{195}Pt resonance ($\delta = -2005$ ppm) occurs ca. 500 ppm downfield with respect to a Pt(II) in a typical N_4 system. The ^{195}Pt downfield shift trend is comparable to that found for heteronuclear Pt−Hg,[47] Pt−Pd,[48] and Pt−Ag [49] complexes where a dative bond Pt → M is proposed. However, in our case it could be postulated that a perturbation of the charge distribution around the metal centers may take place, as a result of a possible Pt···Pt interaction.

Reactivity of 1 toward Oxidation. Due to the short intermetallic Pt···Pt separation found for compound **1**, it was thought **1** could be a good starting compound for the preparation of dimeric species of the type [Pt(II)−Pt(III)]$^+$ (d^8−d^7) and/or [Pt(III)]$_2$ (d^7−d^7) with bond order (BO) of 0.5 and 1 respectively, after oxidation of the initial [Pt(II)]$_2$ (d^8−d^8) species in a one- or two-electron process. Several compounds of this type have been characterized, with the M−M separation being in the same range as that found for **1**: for example, for (d^7−d^7) $K_2[Pt_2Cl_2$-(diphosphite)$_4$] (BO = 1, $d_{Pt-Pt} = 2.695$ (1) Å)[50] and for other platinum species with BO ≠ 0, *cis*-{[$(NH_3)_2$Pt(1−methylthyminato)$_2$PtCl$_2$]$_2$Cl}[PtCl$_6$]·6H$_2$O, (BO = 0.75, $d_{Pt-Pt} = 2.699$ (1) Å),[9d] [Pt$_4$(NH$_3$)$_8$(α-pyrrolidinato)$_4$](NO$_3$)$_6$·3H$_2$O (BO = 0.5, d_{Pt-Pt} = 2.702, 2.709 Å),[51] [Pt$_4$(NH$_3$)$_8$(α-pyrrolidinato)$_4$]-(NO$_3$)$_{5.48}$·3H$_2$O (BO = 0.37, $d_{Pt-Pt} = 2.765$, 2.739, 2.740 Å),[9c] and [Pt$_4$(NH$_3$)$_8$(α-pyridonato)$_4$](NO$_3$)$_5$ (BO = 0.25, d_{Pt-Pt} = 2.779, 2.885 Å).[9a] Nevertheless, our attempts to oxidize **1** with different oxidizing agents such as Ce^{4+}/H^+,[1b] $S_2O_7^{2-}$, HNO_3/O_2,[9e] H_2O_2/H^+, Cl_2/H_2O[52] in aqueous solution or with $NOBF_4$ in nonaqueous solvents (DMF and CH_3CN at −20 °C)[53] were unsuccessful. The low solubility of **1** in aqueous media cannot be rendered as an explanation of this behavior, since, in DMF (in which **1** is soluble), it is also inert. It appears that the bulk of the methyl groups above the basal Pt coordination plane may prevent nucleophiles or electrophiles from approaching the Pt, and therefore it hinders the oxidation process.

M−M Bonding in [Pt$_2$(μ-mtpo)$_4$]. Some authors discuss the nature of d^8···d^8 interactions, as a result of the hybridization of the metal d_{z^2} orbitals through mixing with s and p_z [54] and also by means of ab initio calculations,[55] concluding that a weak M−M bonding interaction takes place.

The topology of the electronic charge density, $\rho(r)$, as pointed out by Bader,[17] is a faithful mapping of the chemical concepts of atoms, bonds, and structure. The principal topological properties are summarized in terms of its critical points.[17,56] A critical point is characterized by signs of its three principal curvatures of $\rho(r)$. Thus, the nuclear positions behave topologically as local maximums in $\rho(r)$, all curvatures being negative. A saddle point (bond critical point) is found between every pair of nuclei, which are considered to be linked by a chemical bond, with two curvatures negative and one positive, indicating that electronic charge is accumulated between the nuclei. Ring critical points are characterized by a single negative curvature.

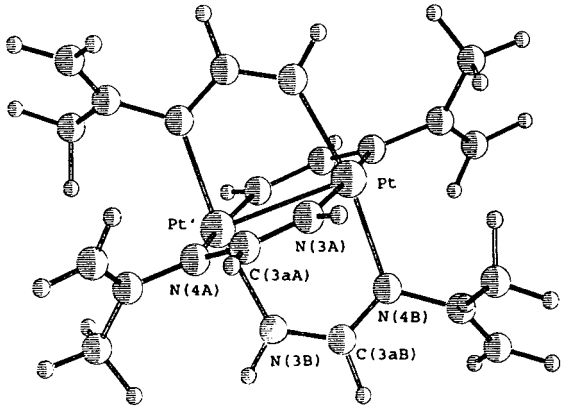

Figure 3. Representation of {Pt$_2$[NHCHN(C(CH$_2$)(CH$_3$)]$_4$} geometrically optimized from ab initio calculations by B3LYP/LANL2DZ method.

Moreover, the Laplacian of $\rho(r)$, $\nabla^2\rho(r)$, determines two extreme situations, where ρ is locally concentrated ($\nabla^2\rho(r) < 0$) and locally depleted ($\nabla^2\rho(r) > 0$). Thus, a value of $\nabla^2\rho(r) < 0$ at a bond critical point is unambiguously related to a covalent bond, showing that a sharing of charge has taken place. However, in a closed-shell interaction a value of $\nabla^2\rho(r) > 0$ is expected, such as found in noble gas repulsive states, in ionic bonds, in hydrogen bonds, and in van der Waals molecules. The last type of interaction is dominated by requirements of the Pauli exclusion principle. Thus, for closed-shell interaction $\rho(r)$ is relatively low and $\nabla^2\rho(r) > 0$.

Furthermore, Bader defined a local electronic energy density, $E_d(r)$, as a functional of the first order of the density matrix

$$E_d(r) = G(r) + V(r)$$

where $G(r)$ and $V(r)$ correspond to a local kinetic energy density and a local potential energy density.[17] The sign of $E_d(r)$ determines whether accumulation of charge at a given point r is stabilizing ($E_d(r) < 0$) or destabilizing ($E_d(r) > 0$). Furthermore, a value of $E_d(r) < 0$ at a bond critical point shows a significant covalent contribution and therefore a lowering of the potential energy associated with the concentration of charge between the nuclei. Also, very recently, Grimme[57] has found for some saturated and unsaturated hydrocarbons a linear correlation between the bond energies, the local electronic energy density, E_d, and ρ at the position of the bond critical points, thus imaging easily the bond energies in molecule.

In a recent paper, we have discussed the nature of the M−M bonding interactions in a Ag(I) dimer in terms of the Bader theory,[38b] and now we present the results concerning the study of the possible bonding nature of the Pt···Pt interaction for [Pt$_2$(μ-mtpo)$_4$]. Thus, the results of ab initio calculations on the model dimer {Pt$_2$[NHCHN(C(CH$_2$)(CH$_3$))]$_4$} (see Figure 1b) are presented. This system was chosen since it resembles the most important features of [Pt$_2$(μ-mtpo)$_4$], differing mainly in its rigidity.

Firstly, a geometry optimization of the model system was carried out, taking the crystallographic geometry as a starting point by means of ab initio MO calculation. The calculations were made using the RHF and DFT (B3LYP) methods with LANL2DZ basis sets, which include relativistic effects and in addition for the latter case electron correlation. Thus, in Table

(46) (a) Albinati, A.; Pregosin, P. S.; Wombacher, F. *Inorg. Chem.* **1990,** *29,* 1812. (b) Frommer, G.; Lianza, F.; Albinati, A.; Lippert, B. *Inorg. Chem.* **1992,** *31,* 2434.
(47) Krumm, M.; Zangrando, E.; Randaccio, L.; Menzer, S.; Danzmann, A.; Holthenrich, D.; Lippert, B. *Inorg. Chem.* **1993,** *32,* 2183.
(48) Krumm, M.; Zangrando, E.; Randaccio, L.; Menzer, S.; Lippert, B. *Inorg. Chem.* **1993,** *32,* 700.
(49) Holthenrich, D.; Krumm, M.; Zangrando, E.; Pichierri, F.; Randaccio, L.; Lippert, B. *J. Chem. Soc., Dalton Trans.* **1995,** 3275.
(50) Che, C.-M.; Herbstein, F. H.; Schaefer, W. P.; Marsh, R. E.; Gray, H. B. *J. Am. Chem. Soc.* **1983,** *105,* 4604.
(51) Matsumoto, K.; Fuwa, K. *J. Am. Chem. Soc.* **1982,** *104,* 897.
(52) Müller, G.; Riede, J.; Beyerle-Pfnür, R.; Lippert, B. *J. Am. Chem. Soc.* **1984,** *106,* 7999.
(53) Ambach, E.; Beck, W. *Z. Naturforsch* **1985,** *48b,* 288.
(54) (a) Mann, K. R.; Gordon, J. G.; Gray, H. B. *J. Am. Chem. Soc.* **1975,** *97,* 3553. (b) Mealli, C.; Pichierri, F.; Randaccio, L.; Zangrando, E.; Krumm, M.; Holtenrich, D.; Lippert, B. *Inorg. Chem.* **1995,** *34,* 3418.
(55) Novoa, J. J.; Aullón, G.; Alemany, P.; Alvarez, S. *J. Am. Chem. Soc.* **1995,** *117,* 7169.
(56) Bader, R. F. W. *Chem. Rev.* **1991,** *91,* 893.
(57) Grimme, S. *J. Am. Chem. Soc.* **1996,** *118,* 1529.

Table 3. Charge Density, ρ, Laplacian $\nabla^2\rho$, Curvatures of ρ (λ_1, λ_2, λ_3), and Bond Ellipticity ($\epsilon = \lambda_2/\lambda_1$), for Model Compound {Pt2[NHCHN(C(CH_2)(CH_3))]$_4$} from RHF/LANL2DZ and B3LYP/LANL2DZ Calculations

	ρ, e/bohr^3	$\nabla^2\rho$, e/bohr^5	λ_1, e/bohr^5	λ_2, e/bohr^5	λ_3, e/bohr^5	ϵ
			RHF/LANL2DZ			
Pt−Pt′	0.051	0.157	−0.041	−0.041	0.239	0.0001
Pt−N(3A)	0.102	0.458	−0.092	−0.062	0.613	0.466
Pt−N(3B)	0.102	0.458	−0.092	−0.062	0.613	0.466
Pt−N(4A)′	0.097	0.431	−0.087	−0.058	0.577	0.500
Pt−N(4B)′	0.097	0.431	−0.087	−0.058	0.577	0.500
ring 1[a]	0.015	0.081	−0.010	0.034	0.057	
ring 2[b]	0.015	0.081	−0.010	0.034	0.057	
			B3LYP/LANL2DZ			
Pt−Pt′	0.056	0.139	−0.041	−0.041	0.221	0.003
Pt−N(3A)	0.117	0.426	−0.113	−0.094	0.634	0.199
Pt−N(3B)	0.117	0.426	−0.113	−0.094	0.634	0.199
Pt−N(4A)′	0.104	0.389	−0.103	−0.085	0.578	0.209
Pt−N(4B)′	0.104	0.389	−0.103	−0.085	0.578	0.209
ring 1[a]	0.016	0.082	−0.010	0.037	0.055	
ring 2[b]	0.016	0.082	−0.010	0.037	0.055	

[a] Ring 1 = Pt−C(3AB)−Pt′. [b] Ring 2 = Pt−C(3AA)−Pt′.

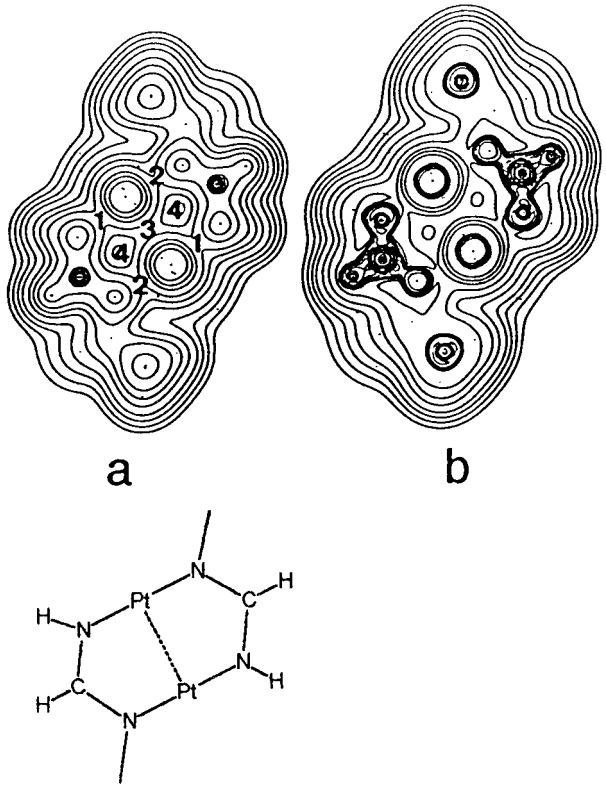

Figure 4. Contour map of ρ (a) and its Laplacian (b) for the plane containing one of the −Pt−N−C−N−Pt−N−C−N− rings derived from ab initio calculations by the B3LYP/LANL2DZ method for {Pt_2[NHCHN(C(CH_2)(CH_3))$_4$}, where 1 = Pt−N3 bond critical points, 2 = Pt−N4 bond critical points, 3 = the Pt−Pt bond critical point, and 4 = the ring critical point.

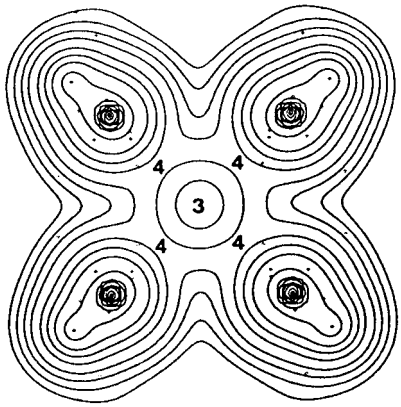

Figure 5. Contour map of ρ for the plane through C3AA, C3AB, C3AA′, and C3AB′, where 3 = the Pt−Pt bond critical point and 4 = the ring critical point.

2 a comparison between the experimental X-ray geometry and the optimized geometries with RHF and B3LYP methods is shown. In Figure 3 the minimized system for B3LYP method is presented. The Pt···Pt separation is almost the same as that found for [Pt_2(μ-mtpo)$_4$], and the Pt−N distances obtained using both methods are also comparable. However, the B3LYP method which takes into account electron correlation gives the most accurate results.

Since in the model system the C(CH_2)(CH_3) group is free to rotate, the steric hindrance is lower than in [Pt_2(μ-mtpo)$_4$].

The contour map of the electronic charge density and its Laplacian for {Pt_2[NHCHN(C(CH_2)(CH_3))$_4$}] in the mean plane through one of the two eight-membered −Pt−N−C−N−Pt−N−C−N− rings as calculated by the AIMPAC program[29] using the B3LYP/LANL2DZ method are shown in Figure 4. The charge density exhibits local maxima only at the position of the nuclei, whereas saddle points (bond critical points) exist between the platinum atoms and each of its bonded nitrogens (points 1 and 2, $\rho_1 = 0.117$ e·bohr^{-3}, and $\rho_2 = 0.104$ e·bohr^{-3}). An extra bond critical point (3) is located between the two platinum atoms with $\rho_3 = 0.056$ e·bohr^{-3}, half the value found for the Pt−N bonds. Such bond critical points and the existence of a zero flux surface for ρ separating the basins corresponding to the platinum atoms (bond path) are indicative of direct metal−metal contact, taking into account that all topological analyses have been done at a minimum on the potential surface.

The laplacian of the charge density is positive at this region (Figure 4b), as expected for closed-shell interaction, as it is for the Pt−N bonds.

However, a value of $E_d < 0$ at the Pt−Pt and Pt−N bond critical points ($E_d = -0.0175$, -0.030, and -0.027 hartree·bohr^{-3} for Pt−Pt, Pt−N3, and Pt−N4, respectively) shows a significant covalent contribution in the Pt−N bonds and the bonding nature of the Pt···Pt interaction. Ellipticity of 0.003 and 0.199 for the Pt−Pt and Pt−N bonds, respectively, show that the former bond has cylindrical symmetry, while the latter have some π character.

Furthermore, two ring points, with two positive curvatures at the $Pt_2N_4C_2$ plane and one positive in the perpendicular direction, also appear (points "4"; see Figures 4 and 5 and Table 3).

The topological analysis of the results obtained with the RHF/LANL2DZ method (see Table 3) yields similar conclusions.

Conclusions

We have shown the ability of a *cisplatin* analogue to build a tetrakis-bridged platinum(II) dimer, displaying a very short M−M contact. The ^{195}Pt NMR studies and MO calculations suggest that a significant M−M interaction takes place. The short intermetallic separation must be the result of a mixture of steric demands of the four bridging mtpo ligands and M−M bonding interactions. The existence of a (+3, −1) bond critical point at the middle point of the platinum atoms, which shows a negative value for the associated electronic energy density (E_d), indicates the existence of a stabilizing interaction between the two metal centers.

Furthermore, the unexpected inertness of **1** towards oxidation in spite of the short Pt···Pt contact may be due to the steric effect caused by the methyl groups which hinders its oxidation.

Experimental and theoretical work is in progress in order to study the oxidation of less sterically hindered molecules, and it will be the subject of future reports.

Acknowledgment. The authors thank DGICYT for financial support (Grant No. PB94-0807-CO2) and Laboratorio de Modelizacion y Diseño Molecular (Universidad de Granada) supported by FEDER funds. J.A.R.N. thanks Junta de Andalucía for a doctoral grant and for a short stay at the Dortmund University. We are especially grateful to Prof. B. Lippert from Dortmund University (Germany) for his helpful discussions and suggestions to this manuscript. We are also grateful to Professor R. W. F. Bader for a copy of the AIMPAC package.

Supporting Information Available: An X-ray crystallographic file in CIF format for compound **2** is available on the Internet only. Access information is given on any current masthead page.

IC960496E